

Above-threshold ionization spectra asymmetrically broadened in the extreme-ultraviolet pulse train and infrared laser fields

Li-Feng Wang,¹ Min Liu,¹ Hao Teng,¹ Bing-Bing Wang,¹ Liang-You Peng,^{2,3} Xin-Kui He,¹ Shi-Yang Zhong,¹ Peng Ye,¹ Peng He,^{1,4} Min-Jie Zhan,¹ and Zhi-Yi Wei^{1,*}

¹Beijing National Laboratory for Condensed Matter Physics, Institute of Physics, Chinese Academy of Sciences, Beijing 100190, China

²State Key Laboratory for Mesoscopic Physics and Department of Physics, Peking University, Beijing 100871, China

³Collaborative Innovation Center of Quantum Matter, Beijing, China

⁴School of Physics and Opto-Electronic Engineering, Xidian University, Xian 710126, China

*Corresponding author: zywei@iphy.ac.cn

Received January 7, 2015; accepted February 8, 2015;
posted February 11, 2015 (Doc. ID 231895); published March 3, 2015

We experimentally investigate the atomic ionization process in an extreme-ultraviolet (XUV) pulse train generated by the high-order harmonic generation process and an IR laser field. Compared with the electron spectrum ionized only by the XUV pulse train, the electron energy spectra generated in the two-color field exhibit two characterizations: (1) the spectrum is smoothed in the presence of a weak IR field, and (2) the spectrum is asymmetrically broadened when using an intense IR field. Simulation results based on the frequency-domain theory qualitatively agree with the experimental spectra. We demonstrate that the asymmetrically broadened spectrum could be interpreted by a clear two-step ionization picture: an electron wavepacket is ionized from the atomic ground state by the XUV pulse train, and then the energy of it is asymmetrically changed by absorbing or emitting specific IR photons. © 2015 Optical Society of America

OCIS codes: (270.6620) Strong-field processes; (340.0340) X-ray optics; (260.3230) Ionization.
<http://dx.doi.org/10.1364/JOSAB.32.000540>

1. INTRODUCTION

The electron ionization process from atoms or molecules in a strong laser field is widely investigated as a crucial step in light-matter interaction. In particular, after the first demonstration of the isolated attosecond pulse in the extreme-ultraviolet (XUV) range [1], it is possible to detect the electron dynamics with attosecond resolution. The most widely used method to measure the pulse duration of the isolated attosecond pulse is the attosecond streak camera [2]. In a typical pump-probe experiment, an electron wavepacket is ionized by an isolated XUV pulse from the ground state of a noble atom; then its momentum shifts as a free particle in the presence of a few-cycle (typically 5 fs) IR laser field. A spectrogram can be measured by scanning the delay time between the isolated XUV pulse and the few-cycle IR pulse, where the temporal characterization of the isolated XUV pulse and the IR laser can be retrieved by applying the FROG-CRAB algorithm [3]. Furthermore a lot of important technologies, such as attosecond tunnelling spectroscopy [4] and attosecond transient absorption spectroscopy [5], have been applied in probing ultrafast electron dynamics as the milestones. In 2007, Uiberacker *et al.* reported the real-time observation of light-induced electron tunneling from neon and xenon for the first time. Their approach was proved to be a powerful tool to probe the electron dynamics in atoms and molecules [6].

To date, most experiments of electron ionization dynamics have been performed with the isolated XUV pulse, where the

isolated XUV pulse is used to pump or probe the electron ionization [7–11]. However, in order to obtain an isolated XUV pulse, besides a few-cycle laser pulse with high energy, many special technologies, for instance, the polarization gating [12], the double optical gating [13], and the ionization gating [14], are needed. Compared with the isolated XUV pulse, it is much easier to generate an XUV pulse train by high-order harmonic generation (HHG) with relatively high flux [15]. Recently, efforts have been made in exploring the electron ionization process with XUV pulse trains [16,17]. For example, Johnsson *et al.* experimentally observed the above-threshold ionization (ATI) spectra by using a train of XUV pulses and an IR laser field with intensity of 3.3×10^{13} W/cm², which produced a few low-order ATI electrons. They illustrated a dramatic enhancement of the ATI spectrum when the delay time of the two fields was zero, and explained the broadening of the spectrum by the shift of the contributions from two consecutive electron wavepackets in opposite directions in energy [18]. Spectra generated by the XUV pulse train and a weak IR laser in argon were recorded by Klünder *et al.* [19]. By taking into account the measurement process, the different time delays between electrons promoted from different electronic states were measured. Although experimental results have been obtained with the XUV pulse train [20–22], the physical explanation of the electron ionization process is still an open question.

In this paper we experimentally measured the electron energy spectra generated by the XUV pulse train in the presence

of a sub-10-fs IR laser field, where the train of XUV pulses is obtained by the HHG process. Comparing the electron energy spectra generated with low and high IR intensities, we have found obvious distinctions. In particular, the ATI spectrum is asymmetrically broadened in the strong IR field and the peak of the whole spectrum is shifted by 14 eV, compared with the energy spectrum generated only by the XUV pulse train. In order to analyze this feature, we have presented simulations by using the frequency-domain theory [23]. Based on the simulation results, a classical interpretation is proposed to describe the ionization process. The electron wavepacket is generated by absorbing an XUV photon, and the energy spectrum of it is broadened by assimilating or ejecting specific IR photons, which is determined by the XUV photon energy and the IR intensity.

2. EXPERIMENTAL RESULTS

A sketch of the experimental system is shown in Fig. 1. A commercial Ti:sapphire laser system (Femtolaser Compact PRO) based on chirped pulse amplification (CPA) technology delivers 25 fs, 0.8 mJ laser pulses at 1 kHz repetition rate. The beam is then focused into a 100 cm fused silica hollow fiber with an inner diameter of 250 μm . A beam pointing system is applied to stabilize the laser incident position into the differentially pumped fibers for a long time. After interacting with the neon, the laser spectrum is broadened, covering 450–950 nm. With a set of chirped mirrors and optics, such as the inset of the wedge, CEP stabilized sub-10-fs laser pulses up to 0.35 mJ are obtained [24].

The system used to record the electron energy spectra is shown in Fig. 2(a). The experimental process is as follows. First, the IR laser pulse is focused into a 2 mm length gas target filled with argon to generate an XUV pulse train by HHG; then the XUV beam and the resident IR laser are focused into a second argon gas jet by an inner Mo/Si multilayer mirror and an annular silver-coated mirror, respectively, with the same focal length of 125 mm [as shown in Fig. 2(c)]. Finally, the ionized electrons are detected by a time-of-flight (TOF) spectrometer. The inner Mo/Si mirror is mounted on a PZT stage, which can control the delay between two beams with a resolution of 330 as. In the experiment, argon is ejected from the gas jet with an inner diameter of 20 μm to form a well-defined interaction volume, and the gas pressure is contained around 7×10^{-4} Pa in the TOF spectrometer to avoid the space charge effect. As shown in Fig. 2(b), a motorized iris in the system is used to control the IR intensity in the interaction volume, and

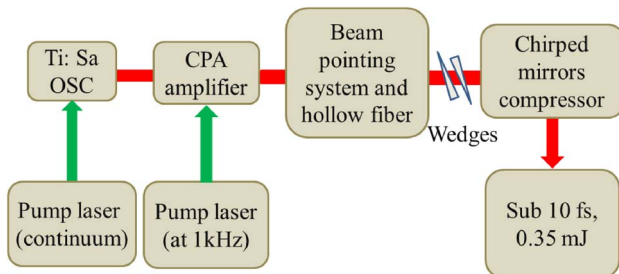


Fig. 1. Sketch of laser system: CPA, chirped pulse amplification. The output spectrum of the 25 fs laser pulses is broadened in the hollow fiber and then compressed to sub-10-fs with wedges and chirped mirrors.

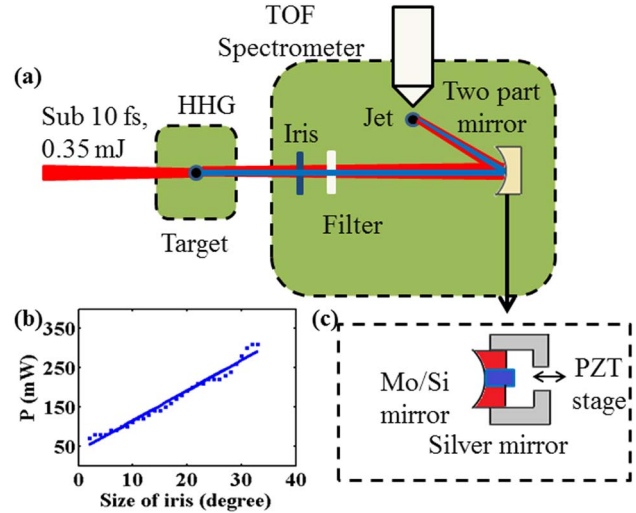


Fig. 2. (a) Setup for detection of electron energy spectrum and (b) power before two-part mirror [details can be found in (c)] versus size of iris without Al filter.

an Al filter with thickness of 300 nm can be added to block the IR laser pulse reflected by the inner Mo/Si mirror. The evaluated IR intensity could be controlled from 2×10^{12} to 6×10^{13} W/cm². The delay between IR and XUV is set at zero in this work [25].

Figures 3(a) and 3(b) present the experimental results of electron energy (E_{kin}) distributions generated by the IR and XUV laser fields, where $E_{\text{kin}} = 10$ –30 eV. Because of the low flux of the XUV beam, the electron is ionized by the single-photon process; hence the XUV photon energy can be estimated by the electron spectrum shown in the inset of Fig. 3(a), where the range of the XUV photon energy is from 24 to 36 eV. When the IR field is weak (3.0×10^{12} W/cm²), almost no electrons can be ionized by IR itself. However, the shape of the spectrum by the XUV plus IR two-color laser field shown in Fig. 3(a) presents a smooth profile compared with the spectrum by only the XUV pulse train. This is because of the appearance of the sidebands produced by the weak IR laser. When the intensity of the IR laser field is increased, the electron energy spectrum [the red dotted line in Fig. 3(b)] generated only by IR itself shows a typical structure of high-order ATI, where the IR intensity is estimated around 5.7×10^{13} W/cm² by the cutoff value of the spectrum [26].

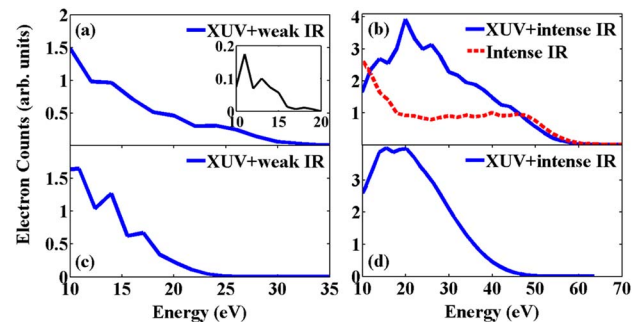


Fig. 3. Experimental electron spectra driven by the XUV pulse train plus IR field at (a) low and (b) high intensities; the inset of (b) illustrates the spectrum generated only by the XUV pulse train. Simulation results are shown in (c) and (d).

With the presence of the XUV pulse train and the strong IR laser field, the electron energy spectrum [solid blue line in Fig. 3(b)] is obviously enhanced and asymmetrically broadened. In particular, the peak of the whole energy spectrum is shifted by 14 eV. This experimental process is different from the standard attosecond streak camera measurement for two reasons. First, the electrons are ionized by the XUV pulse train in our work rather than an isolated XUV pulse in the attosecond streak camera measurement. Second, the IR laser intensity is strong enough to generate high-energy ATI electrons (≥ 10 eV) itself and also to stretch the electron wavepacket ionized by the XUV pulse train in our experiment. However, in the attosecond streak camera measurement, the IR laser intensity should be limited to be strong enough to induce obvious energy shift to the electron wavepacket but not so strong as to generate ATI electrons by itself.

3. ANALYSIS AND DISCUSSION

In order to explain the experimental ATI spectra, we simulate the experimental results by using the frequency-domain theory. Traditionally the theoretical method by solving the time-dependent Schrödinger equation is considered as time-domain theory, where the temporal evolution of the electron wavepacket is obtained by solving the interaction between an electron and a time-dependent electric field. However, in the frequency-domain theory, the laser field is treated as a quantized field, and the ionization process of an atom in a laser field is obtained by calculating the time-independent transition matrix between two states of the atom-laser system [23,27–29]. When an atom is exposed to a two-color linearly polarized laser field, the Hamiltonian of this atom-laser system can be expressed as $H = H_0 + U(r) + V$, where $H_0 = (-i\nabla)^2/2 + \omega_1 N_1 + \omega_2 N_2$ is the energy operator for a free electron-photon laser system; N_1 and N_2 are the photon number operators of the two fields with frequency ω_1 and ω_1 , respectively; $U(r)$ is the atomic binding potential; and V is the electron photon interaction operator. According to Ref. [30], the initial state $|\psi_i\rangle$ is the direct product of the ground state of the atom and Fock states of the laser mode, while the final state $|\psi_f\rangle$ is the quantized-field Volkov state of an electron in a two-color laser field. The transition matrix from the initial state $|\psi_i\rangle$ to the final state $|\psi_f\rangle$ can be written as

$$T = T_d + T_r, \quad (1)$$

where T_d and T_r correspond to the direct and rescattering ATI processes, respectively.

The simulated results are shown in Figs. 3(c) and 3(d) by assuming an IR field with wavelength of 800 nm and an XUV pulse train (containing $\hbar\omega_{\text{XUV}} = 15\omega_1, 17\omega_1, 19\omega_1, 21\omega_1$, and $23\omega_1$ with intensities of $16 \times 10^9, 13 \times 10^9, 7 \times 10^9, 4 \times 10^9$, and 1×10^9 W/cm²). These parameters are chosen by estimated experimental conditions. The result shown in Fig. 3(c) is calculated by averaging three IR intensities: $1 \times 10^{12}, 3 \times 10^{12}$, and 5×10^{12} W/cm², as well as the result shown in Fig. 3(d) with intensities of $3.2 \times 10^{13}, 4.8 \times 10^{13}$, and 6.4×10^{13} W/cm², which are suitable because the intensity of the IR beam changes in the focal region. Comparing the spectra of Figs. 3(a) and 3(b), one can find that the simulated results are in good agreement with the experimental results.

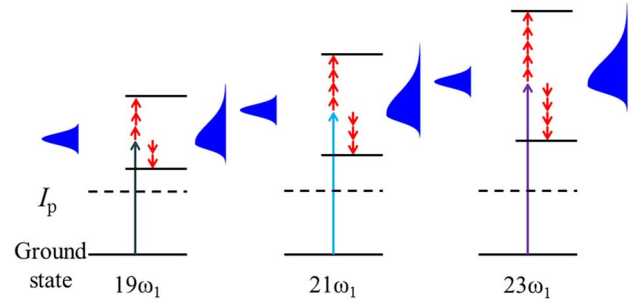


Fig. 4. Sketch of the ionization process in argon driven by three XUV photons ($19\omega_1, 21\omega_1$, and $23\omega_1$) in the presence of IR laser field.

A classical picture can be proposed to explain the behavior of the ionized electron in the IR field after it absorbs one XUV photon. According to Ref. [30], the electron ionization rate depends on the XUV photon energy, and the cutoff energy of the ionized electron can be expressed as

$$\frac{[p_f - eA_{cl}(t_0)]^2}{2} = q_2\omega_2 - I_p, \quad (2)$$

where $A_{cl}(t) = \hat{\epsilon}E_0/\omega_1 \cos(\omega_1 t)$ is the IR laser's vector potential with E_0 being the amplitude of the IR laser's electric field and $\hat{\epsilon}$ being the direction of the laser polarization. By using Eq. (2), the maximum and minimum values of the electron kinetic energy are $E_{\max} = [\sqrt{2(q_2\omega_2 - I_p)} + E_0/\omega_1]^2/2$ and $E_{\min} = [\sqrt{2(q_2\omega_2 - I_p)} - E_0/\omega_1]^2/2$ or 0 (when the XUV photon energy is lower than the ionization potential), respectively. Since the intensity of the XUV pulses is weak in our experiment, one XUV photon absorption dominates the ionization process, i.e., $q_2 = 1$. As shown in Fig. 4, the ionization process driven by the IR and XUV laser pulses can be described by a two-step process. First, one electron wavepacket is ionized into continuum state by one XUV photon absorption. Second, according to Eq. (2), the electron wavepacket absorbs or emits specific IR photons, which induces the

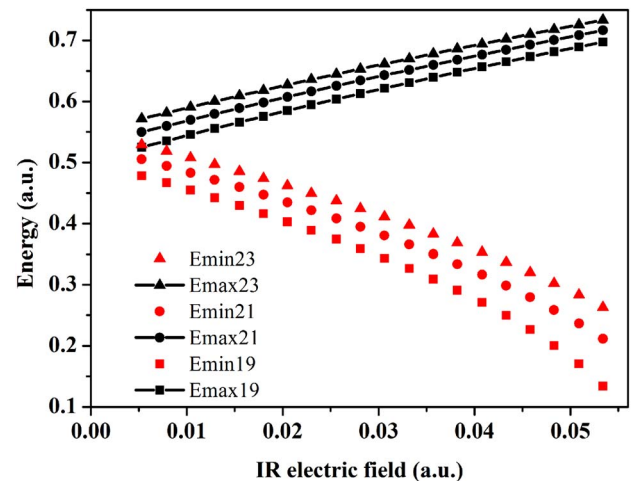


Fig. 5. Comparison of minimum (no line) and maximum (solid line) electron energy excited by three XUV photons in terms of the amplitude of the IR field. Different XUV energy photons are marked by different symbols (squares stand for 19 order, circles stand for 21 order, and triangles stand for 23 order).

spectra asymmetrically broadened in energy. The experimental observation comes from the overlap of all the asymmetrically broadened spectra of electron wavepackets ionized by the broadband XUV pulse train with $\hbar\omega_{\text{XUV}} = 24\text{--}46$ eV. In order to illustrate this broadened spectra quantitatively, comparison of electron energy in terms of the amplitude of the IR field is shown in Fig. 5. For a specific XUV photon, the maximum (minimum) electron energy increases (decreases) with the scale of IR intensity. When the IR intensity is fixed, the maximum and minimum electron energy will increase by the XUV photon energy. From Fig. 5, one can find that the broadening of the spectrum is asymmetric.

4. CONCLUSIONS

In summary, the electron ionization process of argon driven by a two-color field is investigated experimentally, and the ATI energy spectra are measured. The frequency-domain theory is used to find the physical mechanism of the experimental observations. The simulation results are in good agreement with the measured electron energy spectra. The experimental spectra can be explained by a simple physical picture, in which the electron wavepacket is ionized by the XUV pulse train, and then its energy is broadened asymmetrically by the electron absorbing or emitting more IR photons. Our results may be helpful in further applications of XUV pulse trains, such as in the multiphoton ionization process or molecule electron dynamics [31].

ACKNOWLEDGMENTS

This work is partly supported by the National Key Technology R&D Program of the Ministry of Science and Technology (Grant No. 2012BAC23B03), the International Joint Research Program of the National Natural Science Foundation of China (Grant No. 61210017), the National Key Basic Research Program of China (Grant Nos. 2013CB922401 and 2013CB922402), and the National Natural Science Foundation of China (Grant Nos. 11074298 and 11474348).

REFERENCES

- M. Hentschel, R. Kienberger, C. Spielmann, G. A. Reider, N. Milosevic, T. Brabec, P. Corkum, U. Heinzmann, M. Drescher, and F. Krausz, "Attosecond metrology," *Nature* **414**, 509–513 (2001).
- J. Itatani, F. Quéré, G. L. Yudin, M. Y. Ivanov, F. Krausz, and P. B. Corkum, "Attosecond streak camera," *Phys. Rev. Lett.* **88**, 173903 (2002).
- Y. Mairesse and F. Quéré, "Frequency-resolved optical gating for complete reconstruction of attosecond bursts," *Phys. Rev. A* **71**, 011401 (2005).
- F. Krausz and M. Ivanov, "Attosecond physics," *Rev. Mod. Phys.* **81**, 163–234 (2009).
- H. Wang, M. Chini, S. Chen, C.-H. Zhang, F. He, Y. Cheng, Y. Wu, U. Thumm, and Z. Chang, "Attosecond time-resolved autoionization of argon," *Phys. Rev. Lett.* **105**, 143002 (2010).
- M. Uiberacker, Th. Uphues, M. Schultze, A. J. Verhoef, V. Yakovlev, M. F. Kling, J. Rauschenberger, N. M. Kabachnik, H. Schröder, M. Lezius, K. L. Kompa, H.-G. Müller, M. J. J. Vrakking, S. Hendel, U. Kleineberg, U. Heinzmann, M. Drescher, and F. Krausz, "Attosecond real-time observation of electron tunneling in atoms," *Nature* **446**, 627–632 (2007).
- M. Drescher, M. Hentschel, R. Kienberger, M. Uiberacker, V. Yakovlev, A. Scrinzi, T. Westerwalbesloh, U. Kleineberg, U. Heinzmann, and F. Krausz, "Time resolved atomic inner-shell spectroscopy," *Nature* **419**, 803–807 (2002).
- P. Johnsson, J. Mauritsson, T. Remetter, A. L'Huillier, and K. J. Schafer, "Attosecond control of ionization by wave-packet interference," *Phys. Rev. Lett.* **99**, 233001 (2007).
- G. Sansone, F. Kelkensberg, J. F. Prez-Torres, M. F. K. F. Morales, W. Siu, O. Ghafur, P. Johnsson, M. Swoboda, E. Benedetti, F. Ferrari, F. Lpine, J. L. Sanz-Vicario, S. Zherebtsov, I. Znakovskaya, A. L'Huillier, M. Y. Ivanov, M. Nisoli, F. Martn, and M. J. J. Vrakking, "Electron localization following attosecond molecular photoionization," *Nature* **465**, 763–766 (2010).
- A. L. Cavalieri, N. Müller, T. Uphues, V. S. Yakovlev, A. Baltuska, B. Horvath, B. Schmidt, L. Blmel, R. Holzwarth, S. Hende, M. Drescher, U. Kleineberg, P. M. Echenique, F. K. R. Kienberger, and U. Heinzmann, "Attosecond spectroscopy in condensed matter," *Nature* **449**, 1029–1032 (2007).
- M. Schultze, E. M. Bothschafter, A. Sommer, S. Holzner, W. Schweinberger, M. Fiess, M. Hofstetter, R. Kienberger, V. Apalkov, V. S. Yakovlev, M. I. Stockman, and F. Krausz, "Controlling dielectrics with the electric field of light," *Nature* **493**, 75–78 (2013).
- G. Sansone, E. Benedetti, F. Calegari, C. Vozzi, L. Avaldi, R. Flammini, L. Poletto, P. Villoresi, C. Altucci, R. Velotta, S. Stagira, S. De Silvestri, and M. Nisoli, "Isolated single-cycle attosecond pulses," *Science* **314**, 443–446 (2006).
- H. Mashiko, S. Gilbertson, C. Li, S. D. Khan, M. M. Shakya, E. Moon, and Z. Chang, "Double optical gating of high-order harmonic generation with carrier-envelope phase stabilized lasers," *Phys. Rev. Lett.* **100**, 103906 (2008).
- F. Ferrari, F. Calegari, M. Lucchini, C. Vozzi, S. Stagira, G. Sansone, and M. Nisoli, "High-energy isolated attosecond pulses generated by above-saturation few-cycle fields," *Nat. Photonics* **4**, 875–879 (2010).
- H. Mashiko, A. Suda, and K. Midorikawa, "Focusing coherent soft-x-ray radiation to a micrometer spot size with an intensity of 10^{14} W/cm²," *Opt. Lett.* **29**, 1927–1929 (2004).
- R. Buffa, S. Cavalieri, R. Eramo, and M. Matura, "Two color above-threshold ionization: extension to multiple continua," *J. Opt. Soc. Am. B* **13**, 492–495 (1996).
- J. Chen, R. Itakura, and T. Nakajima, "Reconstruction of attosecond pulses using two-color pumping," *J. Opt. Soc. Am. B* **28**, 2195–2199 (2011).
- P. Johnsson, R. López-Martens, S. Kazamias, J. Mauritsson, C. Valentin, T. Remetter, K. Varjú, M. B. Gaarde, Y. Mairesse, H. Wabnitz, P. Salières, P. Balcou, K. J. Schafer, and A. L'Huillier, "Attosecond electron wave packet dynamics in strong laser fields," *Phys. Rev. Lett.* **95**, 013001 (2005).
- K. Klünder, J. M. Dahlström, M. Gisselbrecht, T. Fordell, M. Swoboda, D. Guénot, P. Johnsson, J. Caillat, J. Mauritsson, A. Maquet, R. Taïeb, and A. L'Huillier, "Probing single-photon ionization on the attosecond time scale," *Phys. Rev. Lett.* **106**, 169904 (2011).
- M. Lucchini, K. Kim, F. Calegari, F. Kelkensberg, W. Siu, G. Sansone, M. J. Vrakking, M. Hochlaf, and M. Nisoli, "Autoionization and ultrafast relaxation dynamics of highly excited states in N₂," *Phys. Rev. A* **86**, 043404 (2012).
- J. M. Dahlström, T. Fordell, E. Mansten, T. Ruchon, M. Swoboda, K. Klünder, M. Gisselbrecht, A. L'Huillier, and J. Mauritsson, "Atomic and macroscopic measurements of attosecond pulse trains," *Phys. Rev. A* **80**, 033836 (2009).
- E. Mansten, J. M. Dahlström, J. Mauritsson, T. Ruchon, A. L'Huillier, J. Tate, M. B. Gaarde, P. Eckle, A. Guandalini, M. Holler, F. Schapper, L. Gallmann, and U. Keller, "Spectral signature of short attosecond pulse trains," *Phys. Rev. Lett.* **102**, 083002 (2009).
- B.-B. Wang, L.-H. Gao, X.-F. Li, D.-S. Guo, and P.-M. Fu, "Frequency-domain theory of high-order above threshold ionization based on nonperturbative quantum electrodynamics," *Phys. Rev. A* **75**, 063419 (2007).
- H. Teng, C.-X. Yun, X.-K. He, W. Zhang, L.-F. Wang, M.-J. Zhan, B.-B. Wang, and Z.-Y. Wei, "Observation of non-odd order harmonics by sub-2-cycle laser pulses," *Opt. Express* **19**, 17408–17412 (2011).
- M.-J. Zhan, P. Ye, H. Teng, X.-K. He, W. Zhang, S.-Y. Zhong, L.-F. Wang, C.-X. Yun, and Z.-Y. Wei, "Generation and measurement

- of isolated 160-attosecond XUV laser pulses at 82 eV," *Chin. Phys. Lett.* **30**, 093201 (2013).
26. P. Hansch, M. A. Walker, and L. D. Van Woerkom, "Resonant hot-electron production in above-threshold ionization," *Phys. Rev. A* **55**, R2535(R) (1997).
 27. L.-H. Gao, X.-F. Li, P.-M. Fu, R. R. Freeman, and D.-S. Guo, "Nonperturbative quantum electrodynamics theory of high-order harmonic generation," *Phys. Rev. A* **61**, 063407 (2000).
 28. P.-M. Fu, B.-B. Wang, X.-F. Li, and L.-H. Gao, "Interrelation between high-order harmonic generation and above-threshold ionization," *Phys. Rev. A* **64**, 063401 (2001).
 29. B.-B. Wang, Y.-C. Gao, J. Chen, Z.-C. Yan, and P.-M. Fu, "Frequency-domain theory of nonsequential double ionization in intense laser fields based on nonperturbative QED," *Phys. Rev. A* **85**, 023402 (2012).
 30. K. Zhang, J. Chen, X.-L. Hao, P.-M. Fu, Z.-C. Yan, and B.-B. Wang, "Terrace like structure in the above-threshold-ionization spectrum of an atom in an IR+XUV two-color laser field," *Phys. Rev. A* **88**, 043435 (2013).
 31. X.-R. Liu, Y.-Q. Liu, H. Liu, Y.-K. Deng, C.-Y. Wu, and Q.-H. Gong, "Fully differential measurement on above-threshold ionization of CO and CO₂ molecules in strong laser fields," *J. Opt. Soc. Am. B* **28**, 293–297 (2011).